

# History of on-board equipment improvement for GNSS-A observation with focus on observation frequency

1 **Tadashi Ishikawa<sup>1\*</sup>, Yusuke Yokota<sup>2\*</sup>, Shun-ichi Watanabe<sup>1</sup>, Yuto Nakamura<sup>1</sup>**

2 <sup>1</sup>Hydrographic and Oceanographic Department, Japan Coast Guard, 3-1-1, Kasumigaseki, Chiyoda-  
3 ku, Tokyo, Japan

4 <sup>2</sup>Institute of Industrial Science, University of Tokyo, 4-6-1, Komaba, Meguro-ku, Tokyo, Japan

5 **\* Correspondence:**

6 Tadashi Ishikawa

7 [ishikawa@jodc.go.jp](mailto:ishikawa@jodc.go.jp)

8 Yusuke Yokota

9 [yyokota@iis.u-tokyo.ac.jp](mailto:yyokota@iis.u-tokyo.ac.jp)

10

11 **Keywords: GNSS-A, underwater acoustics, seafloor geodesy, subduction zone, megathrust**  
12 **earthquake**

13 **Abstract**

14 The Global Navigation Satellite System-Acoustic ranging combination technique (GNSS-A) is a  
15 seafloor geodetic technique that enables precise global seafloor positioning to detect subseafloor  
16 geophysical phenomena. The technique requires a sea surface observation platform that combines  
17 GNSS positioning and acoustic ranging. Currently, a survey vessel is used as the platform, which  
18 entails substantial financial and human resources costs, which makes increasing observation  
19 frequency difficult. It is possible to detect long-term average seafloor movement at the centimeter  
20 level, but it is difficult to detect short-term variation due to the insufficiency of observation  
21 frequency. The terrestrial GNSS observation network has detected temporal changes in crustal  
22 deformation fields. These precise observations provide useful information on the megathrust  
23 seismogenic zone. To detect such phenomena on the seafloor, the temporal resolution of the GNSS-A  
24 observation needs to be improved. Advances in vessel equipment technology are crucial for  
25 increasing observation frequency. In this paper, we review the historical development of the Japan  
26 Coast Guard's GNSS-A observation system, focusing on technological developments of on-board  
27 equipment installed on a sea surface platform, and explain how such improvements have increased  
28 observation frequency over time. In the present, ranging frequency has improved from 40-60 s to 15-  
29 20 s by the introduction of the multiple ranging system, resulting in more frequent observations up to  
30 5 times per year for an individual site.

31 **1 Introduction**

32 Space geodetic techniques have been used to monitor crustal deformation. In particular, Global  
33 Navigation Satellite System (GNSS) observation networks have been used to reveal detailed  
34 information from terrestrial crustal deformation fields and discover various geophysical phenomena.  
35 However, to elucidate the physical processes of huge earthquakes that occur around tectonic  
36 subduction zones, it is important to observe crustal deformation on the seafloor just above the focal

37 region. The GNSS-Acoustic ranging combination technique (GNSS-A) was proposed and developed  
38 to extend the GNSS to the seafloor (Spiess, 1985; Asada and Yabuki, 2001; Fujita et al., 2006). This  
39 seafloor geodetic technique has been used to detect various subseafloor geophysical phenomena that  
40 cannot be detected using terrestrial observation and has been providing fruitful knowledge for  
41 geophysics, especially for seismology.

42 The GNSS-A technique has a shortcoming in terms of temporal resolution. Although on-line  
43 continuous observation has been achieved using the GNSS, the GNSS-A can observe only several  
44 times a year in general. Increasing the observation frequency of the GNSS-A is difficult because a  
45 sea surface platform that combines GNSS positioning and acoustic ranging is required. At present, a  
46 vessel is used as the platform, which encompasses substantial operating expenses and human  
47 resources. One of the most important findings from the study of GNSS-A is the detection of huge co-  
48 seismic seafloor displacements due to the 2011 Tohoku-Oki earthquake in Japan (Sato et al., 2011;  
49 Kido et al., 2011). However, because that observation was conducted several weeks after the  
50 earthquake, it is difficult to separate the co- and post-seismic contribution from the observed  
51 displacements. Another important finding from a more recent study is the estimation of the coupling  
52 condition of the plate boundary along the Nankai Trough from GNSS-A-derived inter-seismic  
53 seafloor movement (Yokota et al., 2016). Because the observation is conducted several times a year,  
54 it takes several years to accumulate the data necessary to achieve sufficient accuracy. Therefore, the  
55 plate coupling condition estimated from GNSS-A data is currently only a long-term average value.  
56 Although the terrestrial GNSS network reveals temporal changes in plate coupling (e.g., Ochi, 2015),  
57 it is difficult to detect such phenomena using the GNSS-A. To monitor various geophysical  
58 phenomena more accurately, it is essential to improve the temporal resolution of the GNSS-A.

59 In the last two decades, various slow earthquakes that have the potential to cause huge megathrust  
60 earthquakes have been detected around subduction zones. The relationship between slow earthquakes  
61 and huge earthquakes is an important research topic in the present seismology (e.g., Obara and Kato,  
62 2016). The terrestrial GNSS network has detected long-term slow earthquakes lasting months or  
63 years called slow slip events (SSEs). Recently, GNSS-A has been used to detect SSEs in offshore  
64 regions (Yokota and Ishikawa, 2020). However, GNSS-A lacks the capability to accurately determine  
65 the duration of such events, due to the insufficiency of observation frequency.

66 The ideal solution to improve the temporal resolution of the GNSS-A is continuous observation using  
67 an unmanned sea surface platform instead of a vessel. An unmanned sea surface platform has been  
68 developed by some research groups (Takahashi et al., 2014; Kato et al., 2018), but it has not yet been  
69 put into use for stable observation. It is therefore now important to develop a technology that  
70 increases the frequency of vessel-based observation, which is limited by the high costs associated  
71 with using a ship, including vessel operation time.

72 Advancements in vessel equipment and acoustic ranging technology are indispensable to increase the  
73 observation frequency of the GNSS-A. Since the mid-1990s, we, the Japan Coast Guard research  
74 group, have been developing observation technology to increase the observation frequency and  
75 positioning accuracy. This paper briefly reviews the historical development of the Japan Coast  
76 Guard's observation system.

## 77 **2 GNSS-A observation System**

### 78 **2.1 Basic Concept**

79 Fig. 1a shows a schematic of the GNSS-A observation system. It consists of a sea surface unit and a  
80 seafloor unit. The on-board equipment consists of a GNSS positioning system, an acoustic  
81 transducer, and a dynamic motion sensor set on a surface vehicle. At each site that is surveyed, the  
82 seafloor unit usually consists of four acoustic mirror transponders that are arranged on a rough circle  
83 with its radius equal to the depth of the transponders' placement.

84 The observation system measures the global position of the seafloor transponders according to the  
85 International Terrestrial Reference Frame (ITRF). The position of the GNSS antenna is determined  
86 by baseline kinematic GNSS analysis. In addition to the GNSS positioning, the dynamic motion  
87 sensor records the vessel's attitude. By combining the information on the position of the GNSS  
88 antenna and the vessel's attitude, we can determine the global position of the on-board acoustic  
89 transducer according to the ITRF. The distance between the on-board transducer and the seafloor  
90 transponders are measured by acoustic ranging. Each transponder receives the acoustic signal and  
91 then sends it back to the on-board transducer. The positions of the seafloor transponders are  
92 determined by combining the information on the position of the on-board transducer and the acoustic  
93 signal travel time. In this process, each travel time is converted to distance using an underwater  
94 sound speed profile that is acquired every few hours using temperature and salinity profilers.

### 95 2.2 Acoustic ranging

96 Acoustic ranging is performed to precisely determine the relative position between the on-board  
97 transducer and the seafloor acoustic mirror transponders. As mentioned above, the transponders act  
98 as signal re-transmitters that receive and then return acoustic signals that were sent from the on-board  
99 transducer. In the positioning analysis, correction of underwater sound speed is a key to achieve  
100 centimeter accuracy (Fujita et al. 2006; Yokota et al. 2018). Thus, the installation of multiple  
101 transponders is necessary to accurately estimate perturbations of underwater sound speed (Kido,  
102 2007).

103 The on-board transducer transmits two bi-phase modulation acoustic signals at a carrier wave  
104 frequency of 10 kHz. The first signal is used to identify each transponder and the second is used for  
105 ranging. The sequence code of the modulation used in the system is the maximum length sequence  
106 (M-sequence) code. The 8th and 9th order M-sequence codes are used for the identification and  
107 ranging signals, respectively. One bit of the code consists of four cycles of the carrier wave. Four  
108 phases are repeated 255 times for the identification signal and 511 times for the ranging signal, with  
109 each signal lasting 102.0 ms and 204.4 ms, respectively with 102.0 ms separation. The total time for  
110 one signal including the interval is about 400 ms.

111 As explained above, the seafloor transponder receives the acoustic signals. If the identification signal  
112 code matches that of the transponder, the transponder records the succeeding ranging signal. After a  
113 prescribed interval time set for each transponder, the transponder returns the recoded ranging signal  
114 together with a new identification signal to the sea surface.

115 During the acoustic ranging, the sea surface transducer digitally records both the signals that were  
116 transmitted and received at a sampling frequency of 200 kHz. The precise round-trip travel time is  
117 calculated by cross-correlation between the synthetic signal and the received ranging signal (Asada  
118 and Yabuki, 2001). The onset of the received signal can be identified as the maximum peak in the  
119 correlogram, taking advantage of the characteristics of the M-sequence code. The flow of the  
120 acoustic ranging process is shown in Fig. 2b.

## 121 3 History of changes to the sea surface unit

### 122 3.1 Pole system

123 A schematic of the GNSS-A pole system is shown in Fig. 1a. This early system was used from 2000  
 124 (the first year of our observations) to 2008. The on-board equipment was mounted on a rigid 8-m-  
 125 long pole attached to the stern of the vessel. A GNSS antenna and a motion sensor was attached to  
 126 the top of the pole, and an acoustic transducer was attached to the bottom of the pole. The pole was  
 127 not a permanent fixture and therefore had to be installed for each observation campaign. During  
 128 acoustic measurement, it was necessary to have the bottom of the pole to which the transducer was  
 129 attached extend into the sea. To avoid noise caused by propellers and deformation of the pole due to  
 130 excessive load in the water, acoustic measurement was only possible when the vessel was drifting.  
 131 We initially used an aluminum alloy pole, but in July 2002 we changed to a stiffer stainless steel pole  
 132 to decrease the effects of pole deformation.

133 There were substantial problems with the pole system. The first problem was the difficulty of moving  
 134 the vessel along an ideally balanced line over the transponders. The GNSS-A positioning technique is  
 135 an underwater analogue of GNSS positioning, and the vessel plays the role of the satellite in the  
 136 GNSS. As with the dilution of precision (DOP) of the GNSS positioning due to bad satellite  
 137 geometry, the vessel's track line has a large effect on the accuracy of seafloor positioning. An  
 138 example of the survey line is shown in Fig. 1a. If the entire region above the transponders can be  
 139 covered in a well-balanced manner, then accuracy is maintained, but the data density varies by  
 140 location because the vessel's position during the survey is not well-controlled.

141 Another problem was that observation was inefficient. The time required to transfer the vessel  
 142 between the track lines was almost equal to that required for acoustic measurements (Fig. 1a). In  
 143 addition, human operations on the deck were necessary to move the acoustic transducer up and down  
 144 for vessel transfers. To ensure that deck operations were carried out safely, measurements were  
 145 restricted during the night, and even during the day, measurements were often cancelled because of  
 146 bad weather. Thus, observation took up a lot of ship time in addition to the time required to conduct  
 147 acoustic measurements.

148 Errors in the GNSS-A are mainly caused by variation in the atmosphere/ionosphere along the path of  
 149 the GNSS radio wave and by underwater temperature/salinity along the path of the acoustic wave.  
 150 Because the underwater perturbation has larger spatial and temporal scale than the GNSS-A  
 151 observation time, i.e., several kilometers and hours, it tends to cause systematic bias error for  
 152 positioning. Therefore, developing an analysis method for estimating the underwater conditions in  
 153 detail is an important research target for GNSS-A observation. The method for decreasing systematic  
 154 bias error by estimating the sound speed structure analytically has been developed (e.g., Fujita et al.,  
 155 2006; Ikuta et al., 2008; Yokota et al., 2019). In these models, sufficiently distributed acoustic travel  
 156 time data are needed for sound speed estimation. Specifically, adding the data to to decrease random  
 157 noise errors, several hundreds of acoustic travel time data for each transponder are required. As such,  
 158 the number of acoustic signals that the four transponders were to receive using the pole system was  
 159 empirically set at around 5,000. To obtain a sufficient amount of data, 2-4 days were spent at one  
 160 site. Because a single observation took several days, weather pose problems. Therefore, it was not  
 161 always possible to obtain a sufficient amount of data.

### 162 3.2 Hull-mounted system

163 From 2009, the on-board equipment was permanently mounted on the vessel. In this hull-mounted  
 164 system, the acoustic transducer is attached to the hull and the GNSS antenna is attached to the top of  
 165 the main mast (Fig. 1b). When the vessel is dry-docked, the relative position between the GNSS

166 antenna and the transducer is determined by total stations and GNSS used in terrestrial survey. The  
167 attitude of the vessel is measured by a dynamic motion sensor and used to determine the coordinates  
168 of the transducer relative to those of the GNSS antenna.

169 Measurements are conducted while the vessel moves along an ideal well-balanced track line. In  
170 addition, measurement is possible during both day and night because human operations on the deck  
171 are no longer necessary and there are less interruptions to measurements due to vessel transfer  
172 between track lines compared with the pole system. Thus, measurement accuracy is improved over  
173 that of the pole system (Sato et al. 2013a) and the observation time for a single site is decreased from  
174 2-4 days to 16-24 hours.

175 The required number of acoustic signals was set to about 5,000, as was empirically determined in the  
176 pole system era. However, the hull-mounted system requires less signals because of high efficiency  
177 in obtaining well-balanced data. In 2015, we investigated data collected using the hull-mounted  
178 system and concluded that about 3,500 acoustic signals are enough to take measurements. Thus, the  
179 observation time is decreased to about three quarters.

### 180 **3.3 Hull-mounted system with multiple acoustic ranging**

181 As mentioned above, the on-board transducer transmits two acoustic signals: an identification signal  
182 and a ranging signal. Each transponder has an identification code to distinguish each other and  
183 operates only when receiving the same identification code. Acoustic ranging is conducted by  
184 sequentially transmitting the two signals to four seafloor transponders, with the identification signal  
185 changed to match that of each transponder with each successive attempt (i.e., each cycle). Fig. 2c  
186 shows one cycle of acoustic ranging for four transponders. The signal transmission interval, which  
187 depends on the depth of the transponders, is 10-16 s. Therefore, it takes 40-60 s to complete one  
188 cycle measurement for the transponder array.

189 To increase the observation frequency, it is necessary to decrease the observation time. Thus, a new  
190 transducer called multiple acoustic ranging has been developed that enables multiple transmissions  
191 and receptions in one sequence (Yokota and Okumura, 2015; Yokota et al., 2017). This new  
192 transducer transmits acoustic signals successively without waiting to receive each reply signal from  
193 the seafloor transponders but instead receives all the reply signals at one time (Fig. 2d). In the  
194 conventional system, the ranging signals are all coded using the same M-sequence code. In the new  
195 multiple acoustic ranging system, the ranging signal is coded using different M-sequence codes for  
196 each transponder to avoid crosstalk between receiving signals. Because the ranging signals that are  
197 received have different codes, overlapping signals can be separated by cross-correlation processing.

198 The signal transmission length for one transponder is about 0.4 s and transmission intervals are set to  
199 1 s to protect the internal electric circuit. The length of the transmission sequence takes roughly the  
200 number of transponders multiplied by 1 s. Because the first returned signal arrives before the  
201 transmission of the last signal in the case of shallow transponder depth, the possible number of  
202 transmitted signals depends on the transponder depth. Because the receiving sequence requires a time  
203 length that is enough to receive signals from the farthest transponder, it is set to about 10-16 s  
204 depending on the transponder depth. The entire process takes 15-20 s, which is much shorter than  
205 that of the conventional system, which takes 40-60 s. By measuring the signals from the four  
206 transponders simultaneously in one sequence, the observation is completed in about 3-4 hours, which  
207 is a quarter of that of the conventional system.

## 208 **4 Summary of observation frequency improvement**

209 Fig. 1d shows the time series of the ratio of number of observations to ship operation days and the  
210 average annual observation frequency for each observation system per site. Although there is  
211 variability due to the effects of weather and equipment failure, the graph roughly shows the evolution  
212 of system ability to increase observation frequency.

213 In 2008 and earlier, the pole system era, the ratio was 0.1 - 0.3 and the observation frequency was  
214 about 1 time annually per site. This is insufficient to measure crustal deformations at the centimeter  
215 level. In this era, we increased the observation frequency for seismologically important sites, but  
216 decreased the observation frequency for other sites. In this manner, we succeeded in obtaining the  
217 first seafloor movement velocity at a site off Miyagi where an M7-class earthquake has repeatedly  
218 occurred. Fujita et al. (2006) revealed a high degree of interplate locking offshore Miyagi from the  
219 data of 7 GNSS-A measurements taken during a 3-year period (2002-2005). Matsumoto et al. (2008)  
220 suggested low interplate locking offshore Fukushima.

221 From 2009, the hull-mounted system era, the ratio was improved to 0.5 - 0.6 and the annual  
222 observation frequency was increased to 2-3 times. By optimizing the number of acoustic signals from  
223 5000 to 3500 in 2015, the observation frequency exceeded 3 times as much as that of the pole system  
224 annually per site. Because this frequency is sufficient to measure long-term (4-5 years) movement  
225 rate (i.e., mean velocity) at the centimeter level, it is possible to make observations at the same  
226 frequency for almost all sites. Thus, the spatial heterogeneity of seafloor crustal deformation has been  
227 revealed from wide-area measurement data along the Japan Trench (Sato et al. 2013b) and along the  
228 Nankai Trough (Yokota et al., 2015, 2016).

229 After the installation of the new hull-mounted multi-acoustic ranging system in 2016, the ratio  
230 exceeds 1.0 and the observation frequency is now over 5 times annually per site. In 2017, the  
231 frequency decreased due to electrical failure of the transducer. In the present day, considering the  
232 importance of disaster prevention in the Nankai Trough, we have set the observation frequency for  
233 each site along the Japan Trench and the Nankai Trough to 3 times per year and 4-8 times per year,  
234 respectively. High-frequency observation along the Nankai Trough might disclose temporal changes  
235 of inter-seismic coupling on a yearly basis.

236 In response to seismological demand, short-term geodetic phenomena such as SSEs need to be  
237 detected with certainty. Therefore, increasing the observation frequency of affected sites is essential,  
238 and the development of a new sea surface platform rather than a vessel is required. There are already  
239 studies on a GNSS buoy (Takahashi et al., 2014; Kato et al., 2018) and an automated vehicle  
240 (Chadwell, 2016), but the feasibility of such a system needs to be examined, considering both  
241 operation safety and costs. Also, examination of various possibilities in sea surface platform  
242 engineering will continue to be essential.

### 243 **5 Conflict of Interest**

244 The authors declare no conflict of interest.

### 245 **6 Data Availability**

246 No datasets were used in this study.

### 247 **7 Author Contributions**

248 TI designed the study. YY, TI, and SW led the development of the observation system to increase  
249 observation frequency. TI and YY wrote this manuscript. YY, TI, SW, and YN participated in  
250 discussion about the observation system and made comments to improve the manuscript.

### 251 **8 Funding**

252 The submission of the manuscript was funded by the Japan Coast Guard.

### 253 **9 Acknowledgments**

254 We thank the anonymous reviewers for their helpful comments and suggestions. We thank the many  
255 staff members from the Hydrographic and Oceanographic Department, Japan Coast Guard, including  
256 the crew of the survey vessels Takuyo, Shoyo, Meiyo, and Kaiyo for their support in our  
257 observations and technological developments. We especially thank the active senior staff members  
258 from the Geodesy and Geophysics Office, Hydrographic and Oceanographic Department, Japan  
259 Coast Guard, for their devoted maintenance and management of the equipment.

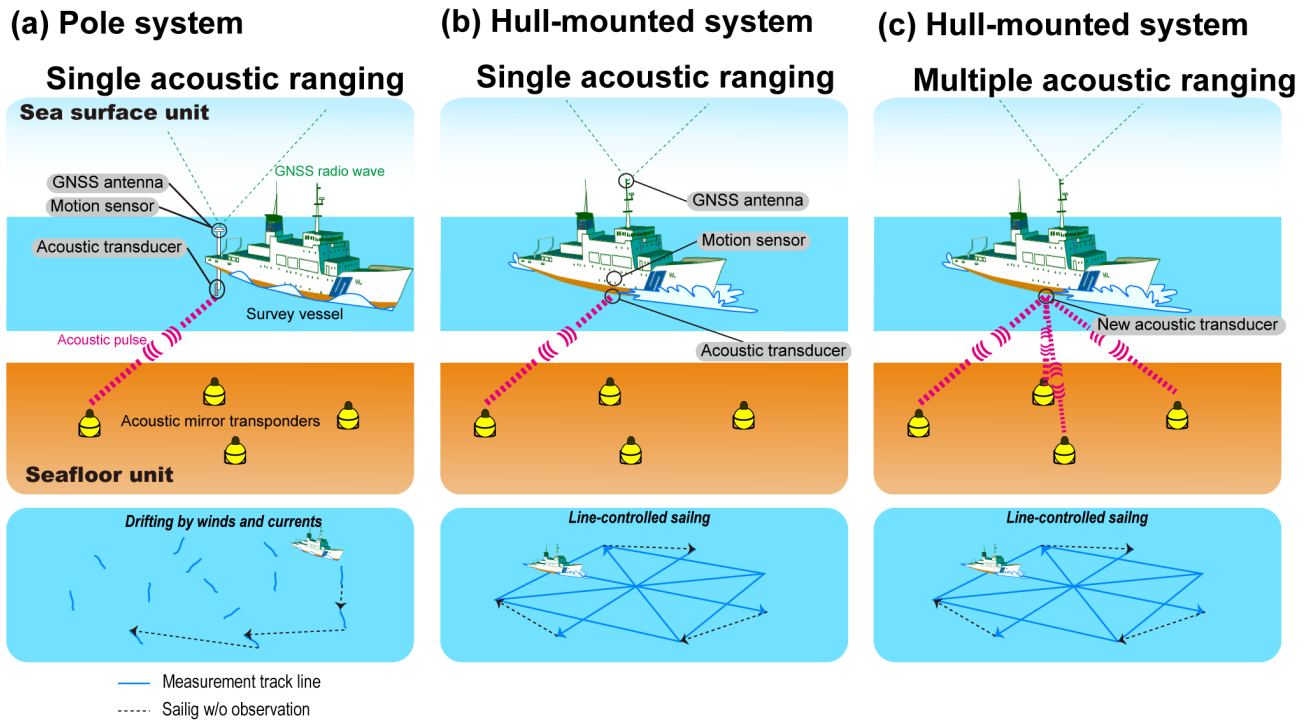
### 260 **References**

- 261 Asada, A., and Yabuki, T. (2001). Centimeter-level positioning on the seafloor. *Proc. Jpn Acad. Ser.*  
262 *B* 77, 7–12. doi:10.2183/pjab.77.7
- 263 Chadwell, C. D. (2016). Campaign-style GPS-Acoustic with wave gliders and permanent seafloor  
264 benchmarks. Subduction Zone Observatory Workshop, Boise Center, Boise, Sep. 29 – Oct. 1  
265 2016.
- 266 Fujita, M., et al. (2006). GPS/acoustic seafloor geodetic observation: method of data analysis and its  
267 application. *Earth Planet. Space* 58, 265–275. doi:10.1007/s00190-013-0649-9
- 268 Ikuta, R., et al. (2008). A new GPS-acoustic method for measuring ocean floor crustal deformation:  
269 Application to the Nankai Trough. *Journal of Geophysical Research*, 113, B02401.  
270 doi:10.1029/2006JB004875
- 271 Kato, T., et al. (2018). Development of GNSS buoy for a synthetic geohazard monitoring system. *J.*  
272 *Disaster Res.* 13, 3, 460–471. doi:10.20965/jdr.2018.p0460
- 273 Kido, M., (2007). Detecting horizontal gradient of sound speed in ocean. *Earth Planet. Space* 59, e33-  
274 e36. doi:10.1186/BF03352027
- 275 Kido, M., Osada, Y., Fujimoto, H., Hino, R., and Ito, Y. (2011). Trench-normal variation in observed  
276 seafloor displacements associated with the 2011 Tohoku-oki earthquake. *Geophys. Res. Lett.*  
277 38:L24303. doi:10.1029/2011GL050057
- 278 Matsumoto, Y., T. Ishikawa, M. Fujita, M. Sato, H. Saito, M. Mochizuki, T. Yabuki and A. Asada  
279 (2008). Weak interplate coupling beneath the subduction zone off Fukushima, NE Japan,  
280 inferred from GPS/acoustic seafloor geodetic observation, *Earth Planets Space*, 60, e9-e12. doi:  
281 10.1186/BF03353114
- 282 Obara, K, and Kato, A. (2016). Connecting slow earthquakes to huge earthquakes, *Science* 353,  
283 6296, 253–257. doi:10.1126/science.aaf1512

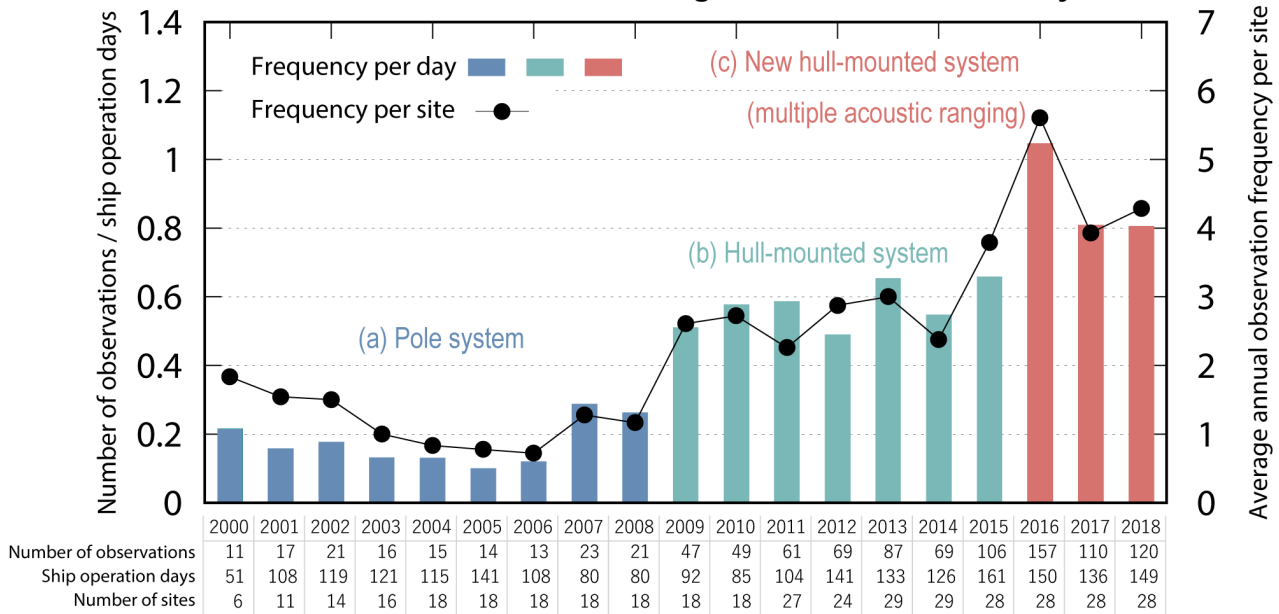


- 284 Ochi, T. (2015). Temporal change in plate coupling and long-term slow slip events in southwestern  
285 Japan, *Earth. Planet. Sci. Lett.*, 431, 8-14. doi:10.1016/j.epsl.2015.09.012
- 286 Sato, M., Ishikawa, T., Ujihara, N., Yoshida, S., Fujita, M., Mochizuki, M., and Asada, A. (2011).  
287 Displacement above the hypocenter of the 2011 Tohoku-oki earthquake. *Science* 332, 1395.  
288 doi:10.1126/science.1207401
- 289 Sato, M., Fujita, M., Matsumoto, Y., Saito, H., Ishikawa, T., and Asakura, T. (2013a). Improvement  
290 of GPS/acoustic seafloor positioning precision through controlling the ship's track line. *J. Geod.*  
291 118, 1–10. doi:10.1007/s00190-013-0649-9
- 292 Sato, M., Fujita, M., Matsumoto, Y., Ishikawa, T., Saito, H., Mochizuki, M., & Asada, A. (2013b).  
293 Interplate coupling off northeastern Japan before the 2011 Tohoku-oki earthquake, inferred from  
294 seafloor geodetic data. *Journal of Geophysical Research: Solid Earth*, 118(7), 3860-3869. doi:  
295 10.1002/jgrb.50275
- 296 Spiess, F. N. (1985). Suboceanic geodetic measurements. *IEEE Trans. Geosci. Remote Sensing GE-*  
297 *23*, 502–510.
- 298 Takahashi, N., Ishihara, Y., Ochi, H., Fukuda, T., Tahara, J., Maeda, Y., et al (2014). New buoy  
299 observation system for tsunami and crustal deformation. *Mar. Geophys. Res.* 35, 243–253.  
300 doi:10.1007/s11001-014-9235-7
- 301 Yokota, Y., and Okumura, M. (2015). Study for improving efficiency in seafloor geodetic  
302 observation by means of multi-acoustic ranging. *Rep. Hydro. Ocean. Res.* 52, 79–87.
- 303 Yokota, Y., et al. (2015). Heterogeneous interplate coupling along the Nankai Trough, Japan,  
304 detected by GPS-acoustic seafloor geodetic observation. *Progr. Earth Planet. Sci.* 2, 10.  
305 doi:10.1186/s40645-015-0040-y
- 306 Yokota, Y., Ishikawa, T., Watanabe, S., Tashiro, T., and Asada, A. (2016) Seafloor geodetic  
307 constraints on interplate coupling of the Nankai Trough megathrust zone. *Nature* 534, 374–377,  
308 doi:10.1038/nature17632
- 309 Yokota, Y., Tashiro, T., and Shimomura, H. (2017). Implementation of multi-acoustic ranging  
310 system. *Rep. Hydro. Ocean. Res.* 54, 32–37.
- 311 Yokota, Y., Ishikawa, T., and Watanabe, S. (2018). Seafloor crustal deformation data along the  
312 subduction zones around Japan obtained by GNSS-A observations. *Scientific Data* 5, 180182.  
313 doi:10.1038/sdata.2018.182
- 314 Yokota, Y., Ishikawa, T., and Watanabe, S. (2019). Gradient field of undersea sound speed structure  
315 extracted from the GNSS-A oceanography. *Marine Geophysical Research*, 40(4), 493-504.  
316 doi:10.1007/s11001-018-9362-7
- 317 Yokota, Y. and Ishikawa, T. (2020), Shallow slow slip events along the Nankai Trough detected by  
318 GNSS-A, *Science Advances*, 6(3), eaay5786. doi: 10.1126/sciadv.aay5786
- 319



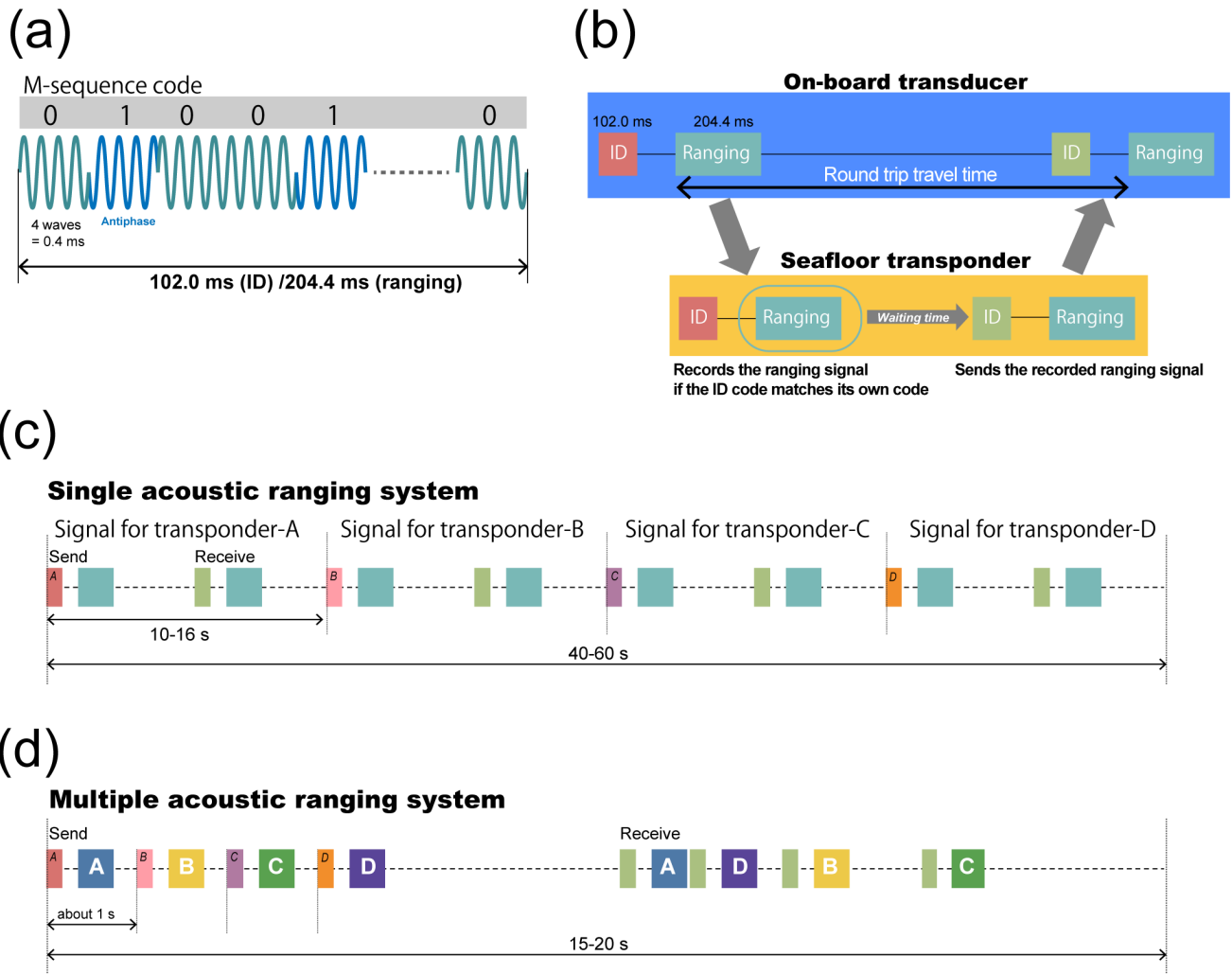


**(d) Changes in observation frequency between 2000 and 2018 with changes to the observation system**



320

321 Figure 1. History of the Japan Coast Guard’s Global Navigation Satellite System-Acoustic ranging  
 322 combination technique (GNSS-A\_ observation system. (a) Schematic of the GNSS-A pole  
 323 system. (b) Schematic of the GNSS-A hull-mounted system. (c) Schematic of the GNSS-A hull-  
 324 mounted system with a new transducer for multiple acoustic ranging. (d) Changes in observation  
 325 frequency between 2000 and 2018 with changes to the observation system.



326

327 Figure 2. Outline of the acoustic ranging system. (a) Acoustic waves coded by four-wave M-  
 328 sequence signals. (b) Flowchart of transmission and reception of acoustic signals. Comparison of  
 329 transmission and reception sequences in (c) the single acoustic ranging system (pole system and  
 330 hull-mounted system) and (d) the multiple acoustic ranging system (new hull-mounted system).  
 331 ID, identification signal.